Supporting Information

Highly Stabilized Silicon Nanoparticles for Lithium Storage *via* Hierarchical Carbon Architecture

Dun Jin,[1#] Balasubramaniam Saravanakumar,[2#] Yuqing Ou,[1] Guanjie Li,[1] Wenguang Zhang,[1] Huirong Wang,[1] Xianfeng Yang[3], Yongcai Qiu,[4,5*] Yuping Wu[1,6] and Weishan Li[1,6*]

[1]School of Chemistry, South China Normal University, Guangzhou 510006, China

[2]School for Advanced Research in Polymers(SARP), Laboratory for Advanced Research in Polymeric Materials (LARPM), Central Institute of Plastic Engineering and Technology (CIPET), B/25, CNI Complex, Patia, Bhubaneswar-751024, INDIA.

[3]Analytical and Testing Centre, South China University of Technology, Guangzhou 510640, China

[4]School of Environment and Energy, South China University of Technology, Guangzhou, 510006, China

[5]State Key Laboratory of Luminescent Materials and Devices, South China University of Technology, Guangzhou, 510006, China

[6]National and Local Joint Engineering Research Center of MPTES in High Energy and Safety LIBs, Engineering Research Center of MTEES (Ministry of Education), and Key Lab. of ETESPG(GHEI), South China Normal University, Guangzhou, 510006, China

[#]They contributed equally to this work

**CORRESPONDING AUTHORS E-mail:* (ycqiu@scut.edu.cn; liwsh@scnu.edu.cn)

Figure S1. The morphological evolution of N-doped CNTs/Si@C.

Figure S2. (a) TEM image and (b-d) corresponding elemental mappings of Si@ZnO.

Figure S3. (a) SEM and (b) TEM images of Si@ZIF-67.

Figure S4. (a) SEM and (b) TEM images of Si@ZIF-67@PDA.

Figure S5. Nitrogen adsorption-desorption isotherm and pore size distribution (inset) of (a) Si@ZIF-67 and (b) Si@ZIF-67@PDA.

Figure S6. XRD patterns of Si@ZIF-67 and Si@ZIF-67@PDA.

Figure S7. (a-c) High-resolution XPS spectra of Si 2p, C 1s and Co 2p of N-doped CNTs/Si@C.

Figure S8. Capacitive contributions to charge storage of N-doped CNTs/Si@C at a scan rate of (a) 0.3 mV s^{-1}, (b) 0.5 mV s^{-1}, (c) 0.8 mV s^{-1}, and (d) 1 mV s^{-1}.

Figure S9. Voltage profiles of the N-doped CNTs/Si@C electrode for different cycles at a current densities of 500 mA g^{-1}.

Figure S10. Voltage profiles of the N-doped CNTs/Si@C electrode for different cycles at a current densities of 1000 mA g^{-1}.

Figure S11. Voltage profiles of the N-doped CNTs/Si@C electrode for different cycles at a current densities of 2000 mA g^{-1}.

Figure S12. Voltage profiles of N-doped CNTs/Si@C electrode under various current densities.

Figure S13. Rate capability of N-doped CNTs/Si@C electrode.

Figure S14. (a) The cycling performance of NCA half cell at 1 C rate (1 C=170 mA g^{-1}) and (b) corresponding charge-discharge profiles.

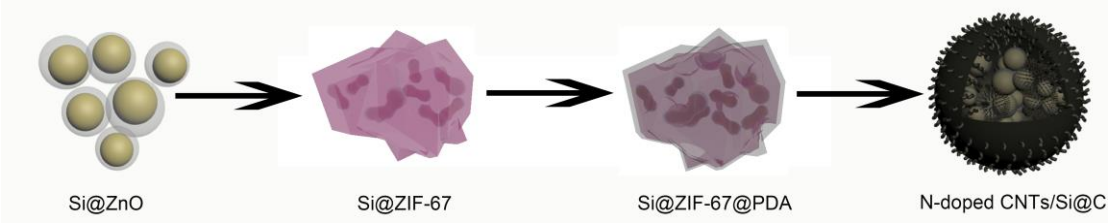

Figure S1. The morphological evolution of N-doped CNTs/Si@C.

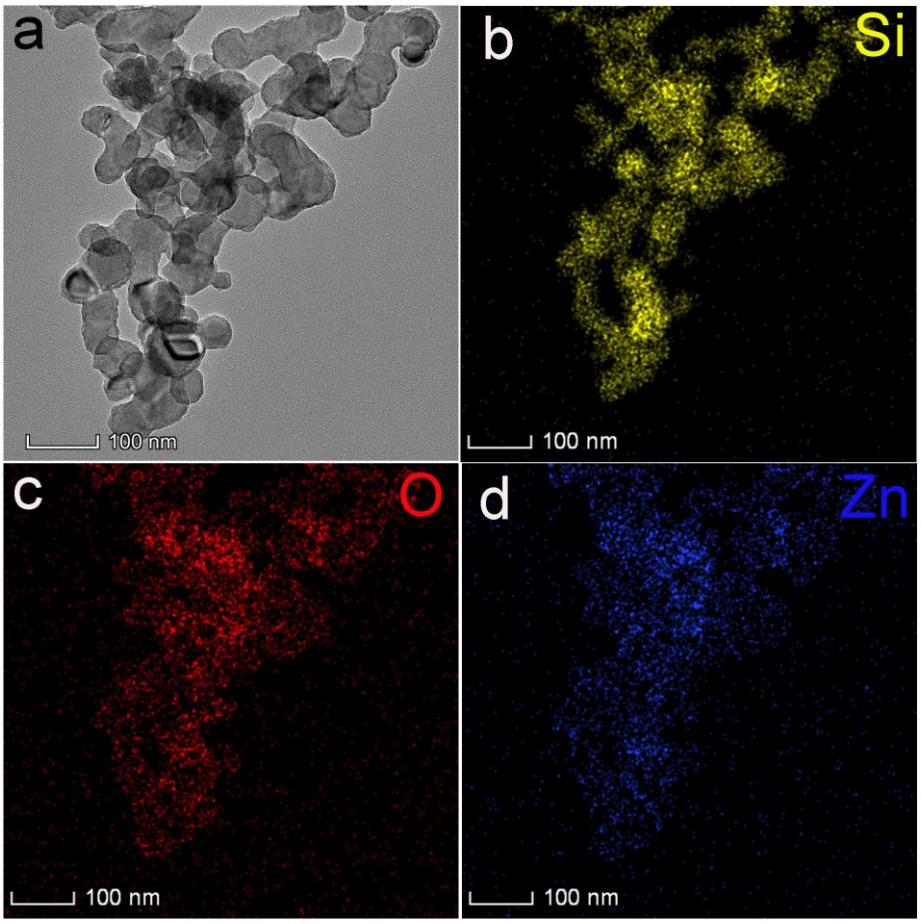

Figure S2. (a) TEM image and (b-d) corresponding elemental mappings of Si@ZnO.

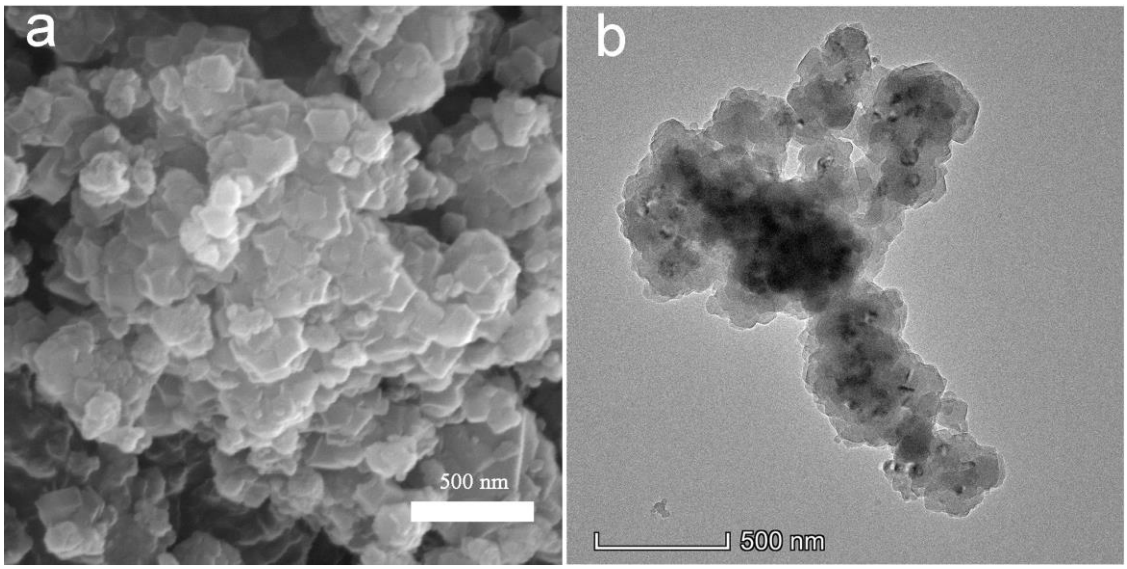

Figure S3. (a) SEM and (b) TEM images of Si@ZIF-67.

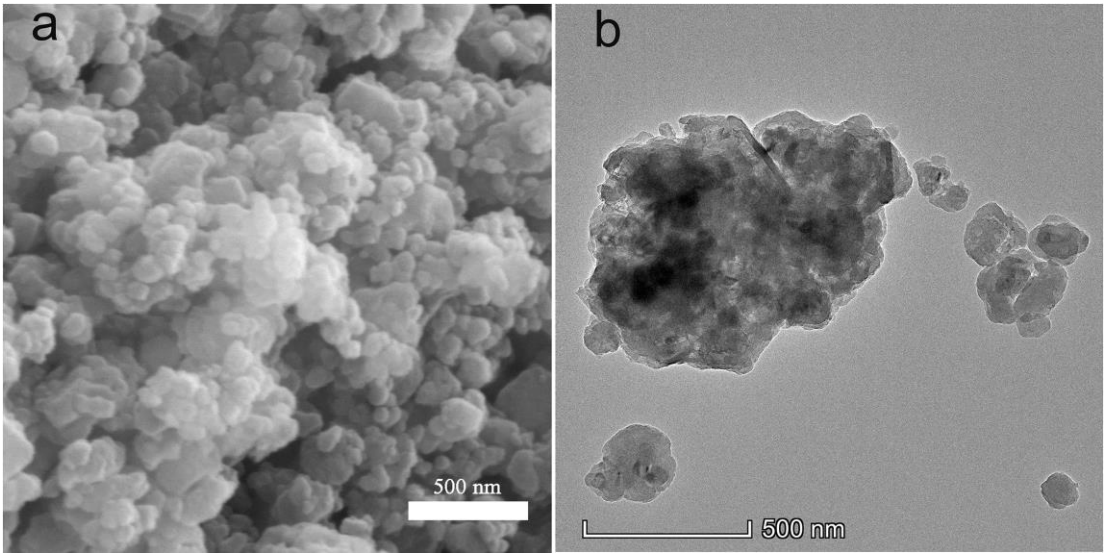

Figure S4. (a) SEM and (b) TEM images of Si@ZIF-67@PDA.

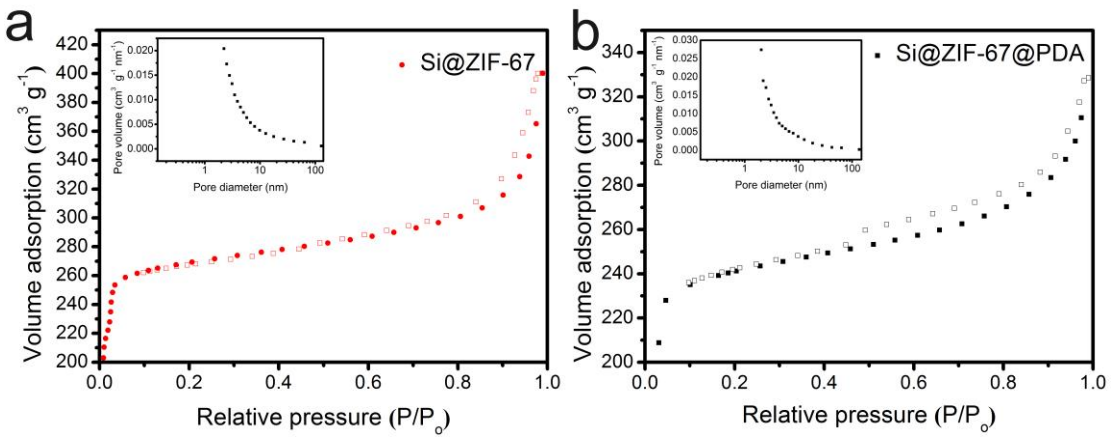

Figure S5. Nitrogen adsorption-desorption isotherm and pore size distribution (inset) of (a) Si@ZIF-67 and (b) Si@ZIF-67@PDA.

S.No	Sample Name	Surface Area (m^2 g^{-1})	Pore Size (nm)
1.	Si@ZIF-67	898	1 -3
2.	Si@ZIF-67@PDA	821	3 - 10
3.	N-doped CNTs/Si@C	234	20 - 30

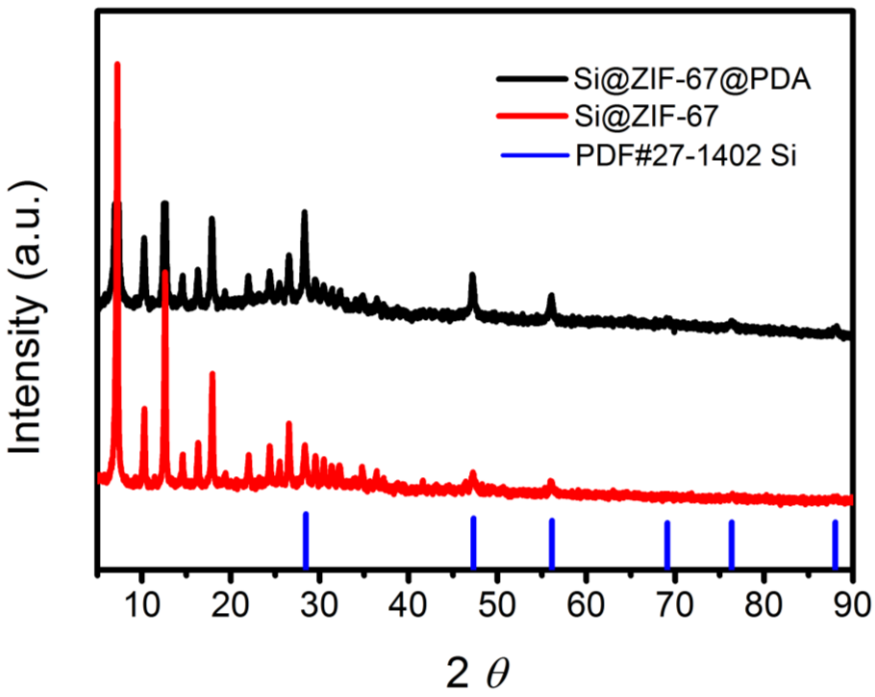

Figure S6. XRD patterns of Si@ZIF-67 and Si@ZIF-67@PDA.

In Figure S6, all diffraction peaks of Si@ZIF-67 match well with both Si phase (JPCDS No. 27-1402) and ZIF-67 phase. There is no obvious change in the XRD pattern of Si@ZIF-67@PDA sample, indicating that the introduction of PDA does not change the crystal structure of the components in Si@ZIF-67 materials.

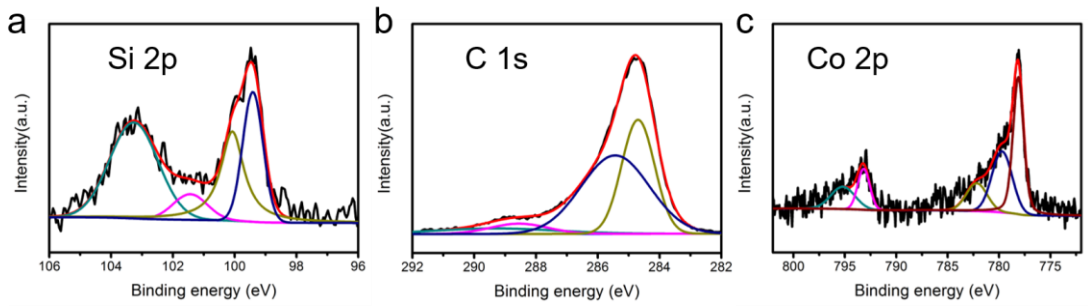

Figure S7. (a-c) High-resolution XPS spectra of Si 2p, C 1s and Co 2p of N-doped CNTs/Si@C.

The Si2p peaks observed around at 103.5 eV and 99.6 eV are assigned to the presence of SiO_x on the Si surface and unoxidized Si atoms, while a weak peak at 101.8 eV belongs to Si-C are observed.[1] 100.3 eV is attributable to SiO_x.[2]

The high-resolution C1s spectrum consists of four peaks centered at 284.7, 286.8, 288.7, and 289.2 eV, corresponding to C-C/C=C,C-OH, C=O/C-N, and -COOH, respectively.[3]

In the high resolution spectrum of Co, the peaks at about 793 eV and 795 eV correspond to Co $2p_{1/2}$, and the peaks at about 778.2 eV 780eV, and 795 eV correspond to Co $2p_{3/2}$.[4]

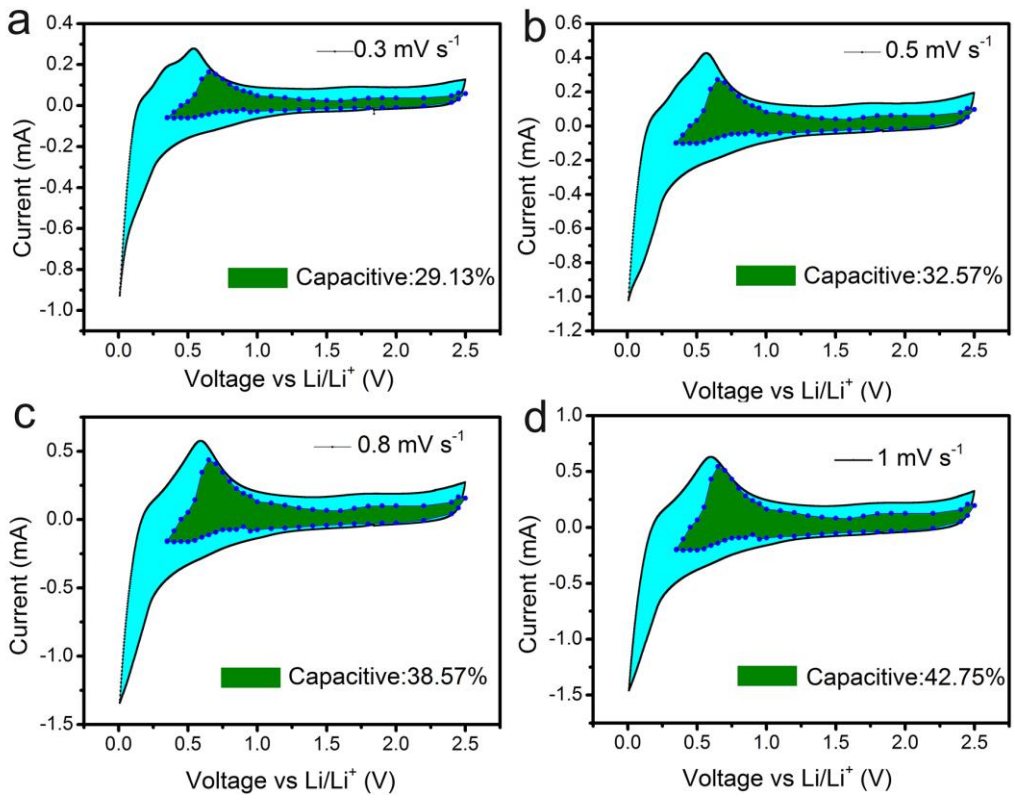

Figure S8. Capacitive contributions to charge storage of N-doped CNTs/Si@C at a scan rate of (a) 0.3 mV s^{-1}, (b) 0.5 mV s^{-1}, (c) 0.8 mV s^{-1}, and (d) 1 mV s^{-1}.

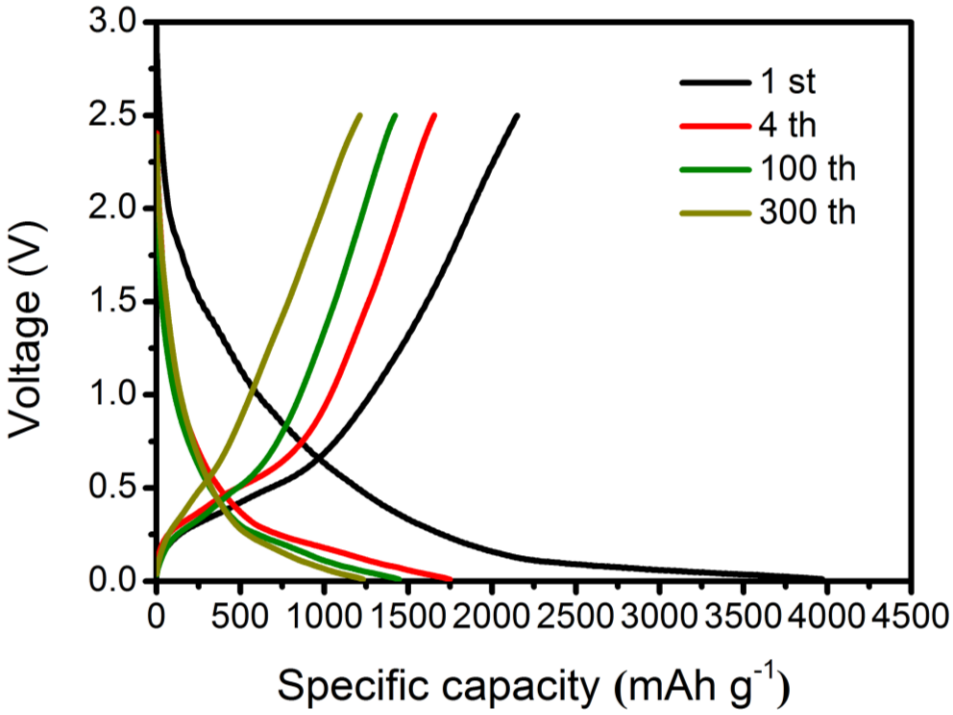

Figure S9. Voltage profiles of the N-doped CNTs/Si@C electrode for different cycles at a current densities of 500 mA g^{-1}.

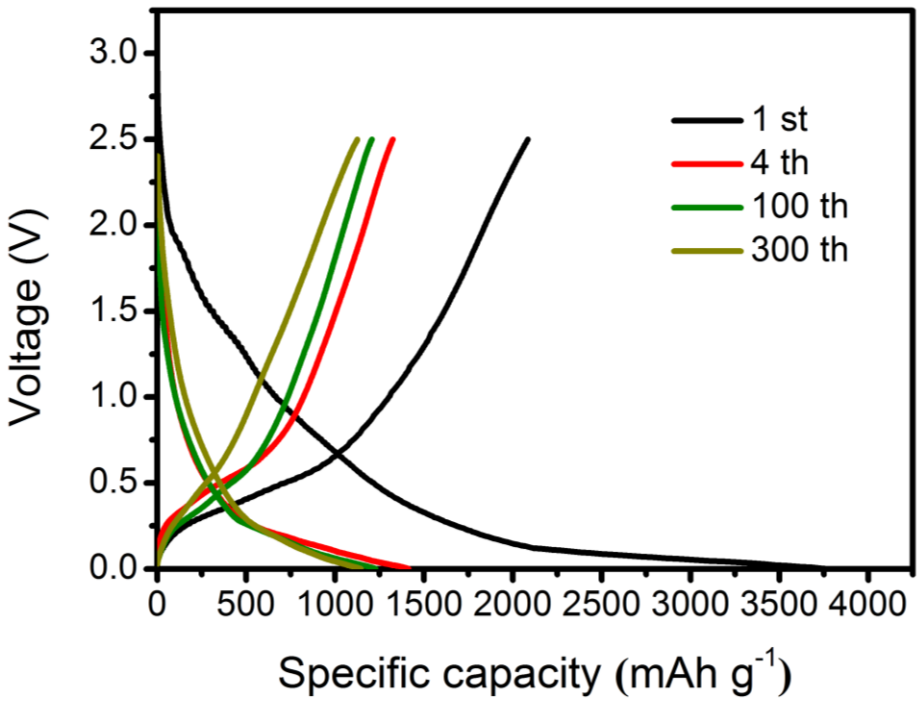

Figure S10. Voltage profiles of the N-doped CNTs/Si@C electrode for different cycles at a current densities of 1000 mA g^{-1}.

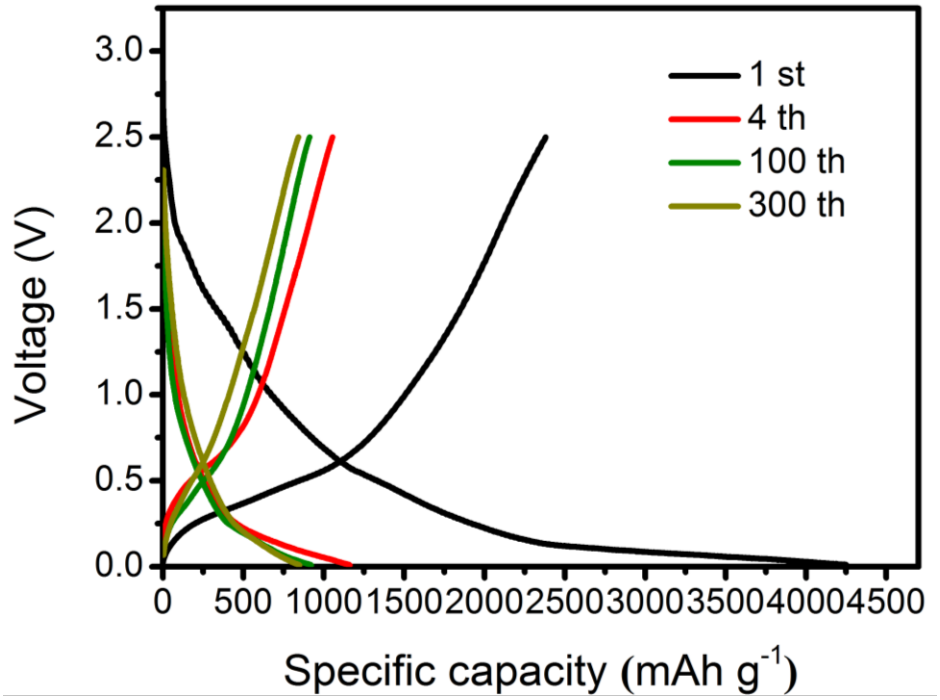

Figure S11. Voltage profiles of the N-doped CNTs/Si@C electrode for different cycles at a current densities of 2000 mA g^{-1}.

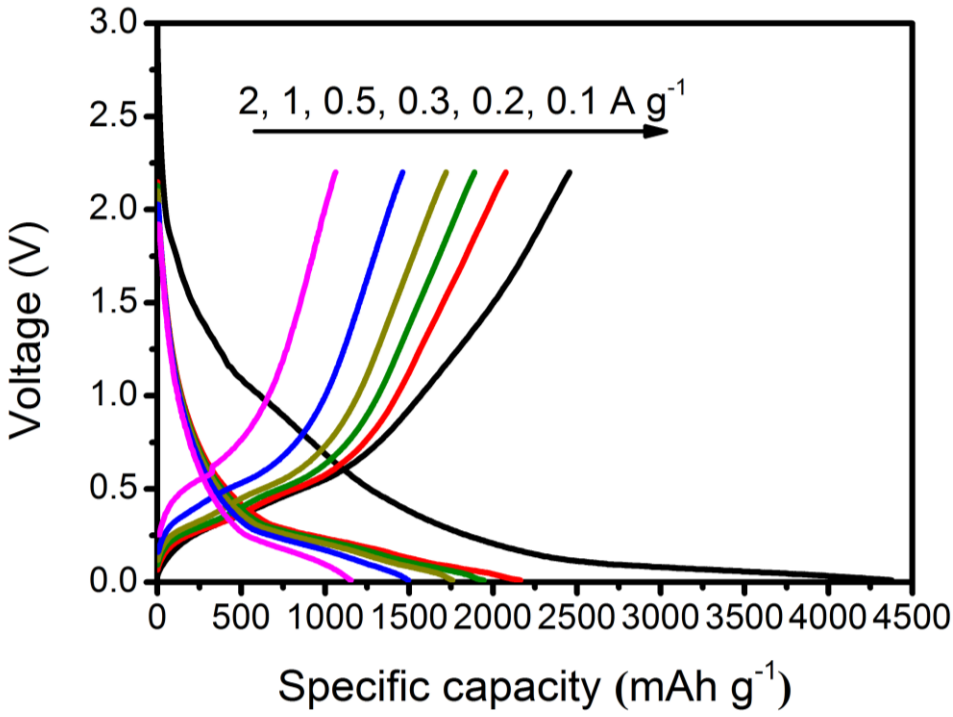

Figure S12. Voltage profiles of N-doped CNTs/Si@C electrode under various current densities.

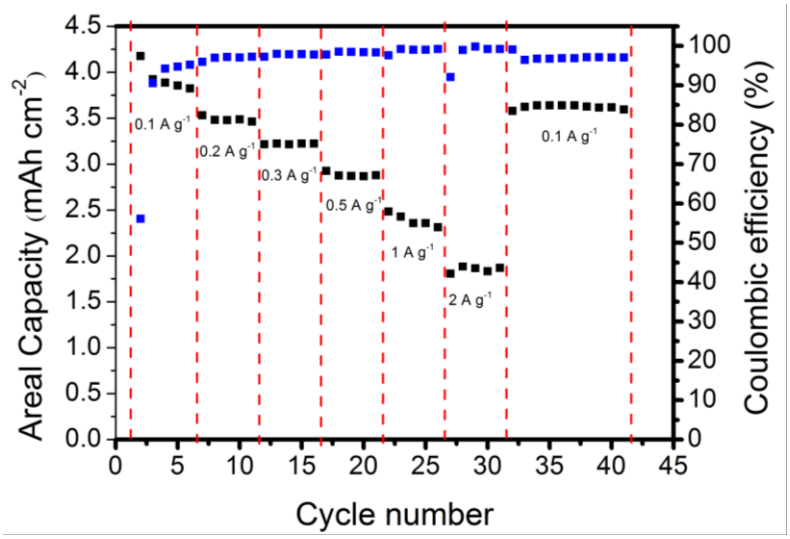

Figure S13. Rate capability of N-doped CNTs/Si@C electrode.

As shown in and Figure S13, the N-doped CNTs/Si@C electrode also shows an excellent rate capability showed a higher areal capacity of about 4.17 mAh cm^{-2}, 3.52 mAh cm^{-2}, 3.21 mAh cm^{-2}, 2.92 mAh cm^{-2}, 2.48 mAh cm^{-2}, and 1.88 mAh cm^{-2} at 0.1 A g^{-1}, 0.2 A g^{-1}, 0.3 A g^{-1}, 0.5 A g^{-1}, 1 A g^{-1}, and 2 A g^{-1}, respectively.

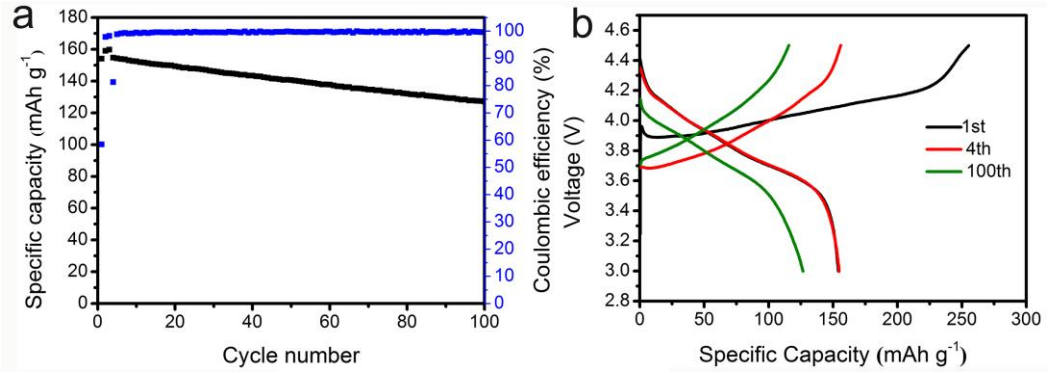

Figure S14. (a) The cycling performance of NCA half cell at 1 C rate (1 C=170 mA g^{-1}) and (b) corresponding charge-discharge profiles.

References

[1] Liu, N.; Liu, J.; Jia, D. Z.; Huang, Y. D.; Luo, J.; Mamat, X.; Yu, Y.; Dong, Y. M.; Hu, G. Z. Multi-core yolk-shell like mesoporous double carbon-coated silicon nanoparticles as anode materials for lithium-ion batteries. Energy Storage Mater., 2019, 18, 165-173.

[2] Sato, K.; Izumi, T.; Iwase, M.; Show, Y.; Morisaki, H.; Yaguchi, T.; Kamino, T. Nucleation and growth of nanocrystalline silicon studied by TEM, XPS and ESR. Appl. Surf. Sci., 2003, 216, 376-381.

[3] Shang, W.; Cai, T.; Zhang, Y. X.; Liu, D.; Liu, S. G. Facile one pot pyrolysis synthesis of carbon quantum dots and graphene oxide nanomaterials: All carbon hybrids as eco-environmental lubricants for low friction and remarkable wear-resistance. Tribol. Int., 2018, 118, 373-380.

[4] Zhang, G. J.; Li, C. X.; Liu, J.; Zhou, L.; Liu, R. H.; Han, X.; Huang, H.; Hu, H. L.; Liu, Y.; Kang, Z. H.; One-step conversion from metal–organic frameworks to Co_3O_4@N-doped carbon nanocomposites towards highly efficient oxygen reduction catalysts. J. Mater. Chem. A, 2014, 2, 8184-8189.